

Coral skeletal carbon isotopes ($\delta^{13}\text{C}$ and $\Delta^{14}\text{C}$) record the delivery of terrestrial carbon to the coastal waters of Puerto Rico

R. P. Moyer · A. G. Grottoli

Received: 29 October 2010 / Accepted: 7 April 2011
© United States Geological Survey 2011

Abstract Tropical small mountainous rivers deliver a poorly quantified, but potentially significant, amount of carbon to the world's oceans. However, few historical records of land–ocean carbon transfer exist for any region on Earth. Corals have the potential to provide such records, because they draw on dissolved inorganic carbon (DIC) for calcification. In temperate systems, the stable- ($\delta^{13}\text{C}$) and radiocarbon ($\Delta^{14}\text{C}$) isotopes of coastal DIC are influenced by the $\delta^{13}\text{C}$ and $\Delta^{14}\text{C}$ of the DIC transported from adjacent rivers. A similar pattern should exist in tropical coastal DIC and hence coral skeletons. Here, $\delta^{13}\text{C}$ and $\Delta^{14}\text{C}$ measurements were made in a 56-year-old *Montastraea faveolata* coral growing ~ 1 km from the mouth of the Rio Fajardo in eastern Puerto Rico. Additionally, the $\delta^{13}\text{C}$ and $\Delta^{14}\text{C}$ values of the DIC of the Rio Fajardo and its adjacent coastal waters were measured during two wet and dry seasons. Three major findings were observed: (1) synchronous depletions of both $\delta^{13}\text{C}$ and $\Delta^{14}\text{C}$ in the coral skeleton are annually coherent with the timing of peak river discharge, (2) riverine DIC was always more depleted in $\delta^{13}\text{C}$ and $\Delta^{14}\text{C}$ than seawater DIC, and (3) the correlation of $\delta^{13}\text{C}$ and $\Delta^{14}\text{C}$ was the same in both coral skeleton and the DIC of the river and coastal waters. These results indicate that coral skeletal $\delta^{13}\text{C}$ and $\Delta^{14}\text{C}$ are recording the

delivery of riverine DIC to the coastal ocean. Thus, coral records could be used to develop proxies of historical land–ocean carbon flux for many tropical regions. Such information could be invaluable for understanding the role of tropical land–ocean carbon flux in the context of land-use change and global climate change.

Keywords Coral geochemistry · $\delta^{13}\text{C}$ · $\Delta^{14}\text{C}$ · Dissolved inorganic carbon · Puerto Rico · Land–ocean carbon flux

Introduction

The transfer of carbon from land to the coastal ocean is an important, but poorly quantified, component of the global carbon cycle. Small mountainous rivers are thought to be major sources of terrestrial carbon input to the world's oceans (e.g., Milliman and Syvitski 1992), and may contribute as much as 33% of the total carbon exported to the coastal ocean in the tropics (Lyons et al. 2002). Most research has focused on large temperate river systems where studies show that the stable- ($\delta^{13}\text{C}$) and radiocarbon ($\Delta^{14}\text{C}$) isotope values of the coastal seawater dissolved inorganic carbon (DIC) pool is influenced by the $\delta^{13}\text{C}$ and $\Delta^{14}\text{C}$ of the dissolved and particulate organic carbon (DOC and POC, respectively) being transported from the adjacent river catchment (Raymond and Bauer 2001; Mayorga et al. 2005; Moyer 2008). Since most studies have been conducted within the last two decades, very few multi-decadal or longer records of land–ocean carbon delivery are available for any region of the Earth. Corals have the potential to provide such records in the tropics because they are long-lived (300 + years), draw on seawater DIC for calcification, and carbon isotopic variations within their skeletons serve as useful proxy records of

Communicated by Geology Editor Prof. Bernhard Riegl

R. P. Moyer (✉)
US Geological Survey, Saint Petersburg Coastal and Marine
Science Center, 600 Fourth Street South, Saint Petersburg,
FL 33701, USA
e-mail: rmoyer@usgs.gov

R. P. Moyer · A. G. Grottoli
School of Earth Sciences, The Ohio State University,
125 South Oval Mall, Columbus, OH 43201, USA

palaeoceanographic variability (Druffel 1997; Gagan et al. 2000; Eakin and Grottoli 2006). Additionally, corals growing in near-shore environments record terrestrial processes, such as increased river discharge and sediment delivery, in their skeletons as fluctuations of elemental barium (McCulloch et al. 2003) or other trace elements (Prouty et al. 2009).

Corals acquire the carbon necessary for skeletogenesis both directly from the DIC in seawater, and indirectly via respiration of photosynthetically and heterotrophically acquired carbon (Grottoli and Wellington 1999; Furla et al. 2000; Grottoli 2002; Hughes et al. 2010). In most shallow-water corals, skeletal $\delta^{13}\text{C}$ is largely influenced by metabolic fractionation effects due to changes in photosynthesis (i.e., changes in light) and heterotrophic rates of carbon acquisition (Swart 1983; Muscatine et al. 1989; Grottoli and Wellington 1999; Grottoli 2002; Swart et al. 2005). Environmental parameters such as cloud cover and light intensity have been shown to influence the value of skeletal $\delta^{13}\text{C}$ (Fairbanks and Dodge 1979; Klein et al. 1992; Grottoli and Wellington 1999; Heikoop et al. 2000; Reynaud-Vaganay et al. 2001; Grottoli 2002). However, since DIC is the ultimate source of skeletal carbon, significant changes in the $\delta^{13}\text{C}$ of ambient seawater DIC should also be reflected in the skeletal $\delta^{13}\text{C}$ of coral skeletons, over and above metabolically driven fractionation in skeletal $\delta^{13}\text{C}$ brought about by changes in light intensity (photosynthesis) or heterotrophy (Swart et al. 2010). The DIC of riverine waters is typically more depleted in $\delta^{13}\text{C}$ than seawater, and thus the input of riverine DIC to the coastal ocean should cause depletions in coastal seawater DIC $\delta^{13}\text{C}$ and coral skeletons. However, due to the seasonal nature and often coincident occurrence of both physical processes which influence the $\delta^{13}\text{C}$ of seawater DIC, and metabolic fractionation of coral skeletal $\delta^{13}\text{C}$, the use of $\delta^{13}\text{C}$ in coral skeletons as a singular tracer of changes in ambient seawater DIC has remained difficult (Swart et al. 1996).

Radiocarbon (^{14}C) enters the ocean through gas exchange of atmospheric CO_2 resulting in surface seawater DIC $\Delta^{14}\text{C}$ values that reflect a combination of the atmosphere's $\Delta^{14}\text{C}$ values and surface ocean processes. In the 1950s and 1960s, thermonuclear weapons testing approximately doubled the "pre-bomb" inventory of ^{14}C in the atmosphere, thereby producing a large increase in surface seawater DIC $\Delta^{14}\text{C}$ as well. Radiocarbon values in coral skeletons have been shown to closely reflect the ^{14}C composition of the seawater DIC in which they are growing, independent of metabolic fractionation effects (Druffel and Linick 1978; Nozaki et al. 1978; Konishi et al. 1982). The $\Delta^{14}\text{C}$ values of riverine and soil pore water DIC is largely derived from the respiration and photo-oxidation of aged terrestrial organic matter (OM), and therefore has

lower $\Delta^{14}\text{C}$ than seawater (e.g., Mayorga et al. 2005). Thus, the input of riverine DIC to the coastal ocean should also produce depletions of $\Delta^{14}\text{C}$ in coastal seawater DIC and coral skeletons.

The use of paired measurements of $\delta^{13}\text{C}$ and $\Delta^{14}\text{C}$ has been shown to be more effective than using either isotope alone for calculating fluxes and residence times of carbon in terrestrial and marine aquatic systems (Raymond and Bauer 2001; Mayorga et al. 2005; Moyer 2008). The goal of this study was to use paired $\delta^{13}\text{C}$ and $\Delta^{14}\text{C}$ measurements in tropical rivers, the coastal ocean, and coral skeletons to show linkages between riverine DIC and the coral skeleton. Using this approach, the following hypotheses were addressed: (1) the influx of $\delta^{13}\text{C}$ - and $\Delta^{14}\text{C}$ -depleted riverine DIC to the coastal ocean results in synchronous depletions in coral skeletal $\delta^{13}\text{C}$ and $\Delta^{14}\text{C}$, and (2) depletions in coral skeletal $\delta^{13}\text{C}$ and $\Delta^{14}\text{C}$ occur during periods of high rainfall and large river discharge (i.e., the wet season).

Materials and methods

Study area

The Fajardo river catchment is located in northeastern Puerto Rico (Fig. 1) and encompasses a total area of $\sim 70 \text{ km}^2$. The largest river within the catchment, the Rio Fajardo, is fed by several smaller streams originating in the Luquillo Mountains and flows seaward in an easterly direction, eventually draining into Vieques Sound (Fig. 1b). A small coral reef, Cayo Ahogado, is located approximately 1 km from the mouth of the Rio Fajardo (Fig. 1b), and is characterized by low percent cover of scleractinian corals, with *Montastraea* sp., *Porites* sp., and *Siderastrea* sp. being the most common. The climate in this region of Puerto Rico exhibits seasonal variability with a wet season during the months of May through mid-January, and a dry season during the months of mid-January through April. Average rainfall in the catchment is $1,592 \text{ mm year}^{-1}$, with peak precipitation occurring in May, October, November and peak river discharge occurring during November.

Coral sampling

On 5 October 2004, a coral core was taken from a 0.63 m tall colony of *Montastraea faveolata* growing on the seaward fore-reef slope of Cayo Ahogado (N $18^\circ 19.413'$; W $065^\circ 37.084'$) at 6 m water depth, using a hand-held submersible pneumatic drill. The selected colony was alive, had no visible signs of major mortality, and did not appear to be undercut by bioerosion at the base of the

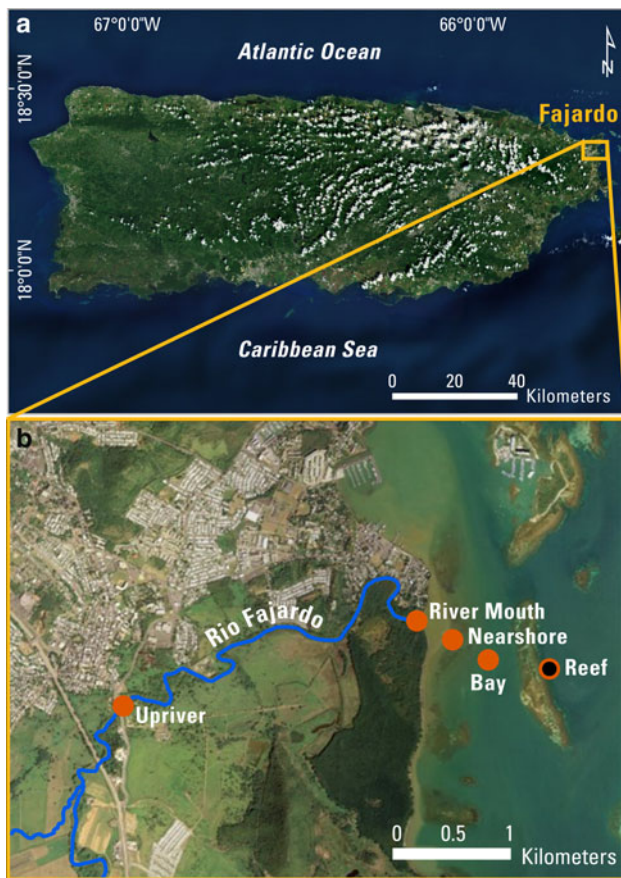


Fig. 1 **a** Landsat 7 image of Puerto Rico, showing the location of the Fajardo study area within Puerto Rico, and **b** USGS 1:24000 aerial image mosaic of the lower Rio Fajardo Catchment. Orange circles indicate water sampling locations and the black circle with orange ring indicates where the Fajardo coral core was collected as well as the water sampling location over the reef at Cayo Ahogado

colony. The Fajardo core was 3 cm in diameter and consisted of four segments totaling 62.5 cm in length. Each core segment was cut longitudinally into ~6-mm-thick slabs, washed with high-pressure deionized water, and dried overnight at 60°C. Core sections were x-radiographed by placing the core slabs on Kodak Industrex AA440 ready-pack film and exposing them to X-rays at 70 kVp and 15 ma for 9.0 s with a source-to-object distance of 1 m. Films were manually developed and negatives were digitized using a single-line medical film scanner. The resulting images were used to determine the growth chronology of the Fajardo core.

When developing the age model, pairs of high- and low-density bands were considered to be annual (Knutson et al. 1972; Dodge and Vaisnys 1975; Hudson et al. 1976), with the high-density portion of each annual band forming in early summer (Watanabe et al. 2002; Kilbourne et al. 2007). Additional constraint on the age model was achieved by comparing $\Delta^{14}\text{C}$ measurements (as described below) with other records available from Atlantic and Caribbean corals

(compiled by Grottoli and Eakin 2007) and ensuring that the chronology developed via counting density bands corresponded to the occurrence of the base and peak of the bomb ^{14}C signature within the Fajardo core. Age models developed via density band counting and $\Delta^{14}\text{C}$ measurements were in very good agreement, and no adjustments were made to the overall chronology based on either method.

The coral skeleton was milled at 1-mm intervals along the major axis of maximum growth using a handheld drill fitted with a diamond dental drill bit, yielding a total of 323 samples (Fig. 2). Additional high-resolution samples were collected at 0.1-mm increments between 5 and 15 mm from the top of the core along the same sampling path (Fig. 2) using a Merchantek Micromill and produced an additional 100 samples. Samples for ^{14}C analysis ($n = 54$) were taken at 1 mm increments where large negative $\delta^{13}\text{C}$ excursions were measured within the coral skeleton. Since larger sample amounts were required for ^{14}C analysis, skeletal material was drilled in a horizontal plane immediately adjacent to the corresponding stable isotope sample path (Fig. 2).

Water sampling

Surface (0.5–1.5 m) river and seawater samples were collected for DIC $\delta^{13}\text{C}$ and $\Delta^{14}\text{C}$ analysis during both the wet (October 2004 and 2007) and the dry seasons (March 2005 and 2008). Samples were collected along a transect in the lower Fajardo catchment and coastal zone at the following locations: up-river, at the river mouth, in the nearshore waters seaward of the river mouth, in the bay at a median distance to Cayo Ahogado, and directly above the coral reef at Cayo Ahogado (Fig. 1b). Each water sample was collected by peristaltic pump, filtered through a pre-baked Whatman QMA filter (0.7 μm pore size), individually stored in pre-cleaned glass bottles, poisoned with mercuric chloride, and sealed with an air-tight rubber seal. Duplicate samples at the up-river and reef locations were collected each season. Full details of the DIC sample collection methods can be found in Moyer (2008).

Stable isotope analyses

Approximately 100 μg of finely ground skeletal powder was acidified at 70°C with 100% H_3PO_4 in an automated Kiel III carbonate sampling device. $\delta^{13}\text{C}$ and $\delta^{18}\text{O}$ of the resulting CO_2 gas were measured with a Finnigan MAT 252 triple collecting stable isotope ratio mass spectrometer (SIR-MS) in Grottoli's laboratory. Only $\delta^{13}\text{C}$ values are presented here and are reported as the per mil (‰) deviation of $^{13}\text{C}/^{12}\text{C}$ relative to the Vienna Pee Dee Belemnite (VPDB) limestone standard (Coplen 1996). The standard deviation (SD) of repeated measurement of an internal

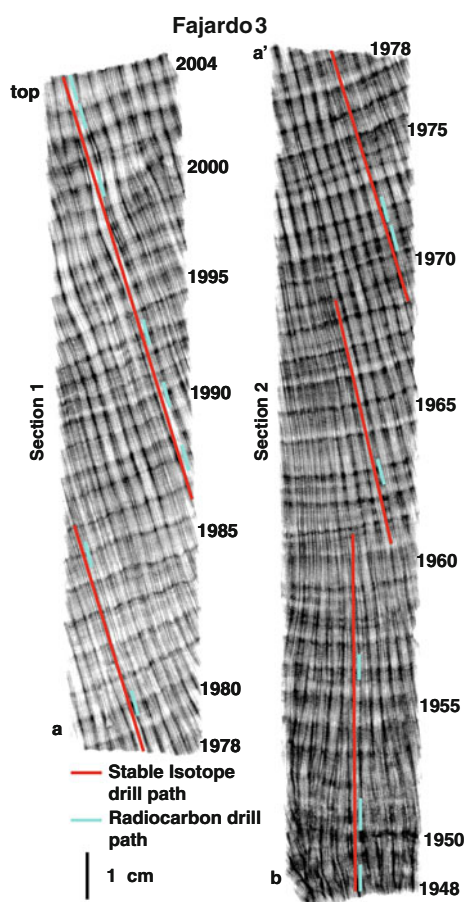


Fig. 2 X-radiograph positive prints of the *top two* sections of the Fajardo coral core. The age model based on annual bands is indicated along the *right side* of each core section. The drill paths for stable (*red line*) and radiocarbon (*blue line*) isotopic analyses are shown

standard ($n = 83$) and duplicate samples ($n = 40$) was $\leq \pm 0.05\%$.

DIC samples were prepared for isotopic analyses using methods described in Moyer (2008). Briefly, each sample was acidified ($\text{pH} < 2$) with 100% H_3PO_4 , sparged under helium flow, and the resulting CO_2 cryogenically purified under vacuum. The CO_2 gas was then split into two glass ampoules: one for $\delta^{13}\text{C}$ and one for $\Delta^{14}\text{C}$ analyses. $\delta^{13}\text{C}$ -DIC measurements were carried out using a multiport gas inlet system connected to a Finnigan Delta Plus IV SIR-MS in Grottoli's laboratory and reported in per mil relative to the VPDB standard. Repeated measurement of a seawater DIC internal laboratory precision standard ($n = 44$) had a SD of $\pm 0.02\%$.

Radiocarbon analyses

Approximately 10 mg of homogenized coral skeletal powder samples were sent to the Keck Accelerator Mass Spectrometer (AMS) facility at the University of California-Irvine for high-precision ^{14}C analysis. Samples were

converted to CO_2 under vacuum with 85% H_3PO_4 , then converted to graphite using an Fe catalyst with H_2 gas as the reducing agent (Vogel et al. 1987). The ratios of $^{14}\text{C}/^{12}\text{C}$ and $^{13}\text{C}/^{12}\text{C}$ were measured using an NEC 0.5 MV compact AMS and background subtraction was applied using ^{14}C -free spar calcite. The SD of all coral $\Delta^{14}\text{C}$ measurements relative to the Oxalic Acid I standard was $\pm 1.7\%$.

DIC samples collected in 2004 and 2005 were sent to the National Ocean Service AMS facility for $\Delta^{14}\text{C}$ -DIC analyses, while samples collected in 2007 and 2008 were sent to the Arizona AMS Laboratory. For both sets of samples, CO_2 gas was converted to graphite using an Fe catalyst and the ratio of $^{14}\text{C}/^{12}\text{C}$ was measured via AMS, with background subtraction applied using ^{14}C -free groundwater. The SD of all $\Delta^{14}\text{C}$ -DIC measurements relative to the Oxalic Acid I standard was $\pm 5.0\%$.

All ^{14}C measurements (coral and DIC) were reported as fraction modern and converted to $\Delta^{14}\text{C}$ (the per mil deviation of $^{14}\text{C}/^{12}\text{C}$ in the sample relative to that of the 95% Oxalic Acid-1 standard) according to the conventions of Stuiver and Polach (1977) for geochemical samples with known age. All $\Delta^{14}\text{C}$ values were corrected for fractionation using the $\delta^{13}\text{C}$ values measured by SIR-MS.

Data analysis

Coral $\delta^{13}\text{C}$ data were compared with the Rio Fajardo historical discharge record (1961–2004) available from the United States Geological Survey (<http://www.pr.water.usgs.gov>, Station 50071000). Prior to analysis, $\delta^{13}\text{C}$ and river discharge time series were detrended by subtracting the long-term linear mean from each data point. Periodicity trends within these individual data sets were examined using single spectrum analysis based on a fast Fourier transform of the co-variance function, and co-variation and correlation between the two stochastic time series was tested for using bivariate cross-spectral analysis. A Hamming window (width = 5) was applied to both time series. Coherency confidence limits were estimated using the methods described by Thompson (1979). All time series analyses were performed using Statistica version 8 (© 2007 StatSoft, Inc.).

The Pearson product-moment correlation coefficient was calculated in order to determine the degree of interdependent covariation between detrended coral $\delta^{13}\text{C}$ and $\Delta^{14}\text{C}$. Coral $\delta^{13}\text{C}$ was detrended as describe above; however, since a single line did not reasonably fit the coral $\Delta^{14}\text{C}$ data, three distinct sections of the bomb ^{14}C signature were considered. A linear mean was subtracted from each of (1) the pre-bomb portion of the record (1948–1956); (2) the mid-record rise of bomb ^{14}C (1956–1972); and (3) the post-bomb portion of the record (1972–2004). Interdependent covariation between coral $\delta^{13}\text{C}$ -DIC and $\Delta^{14}\text{C}$ -DIC was also determined using

Pearson product–moment correlation. Statistical difference between correlations of $\delta^{13}\text{C}$ and $\Delta^{14}\text{C}$ in coral skeleton and the DIC of ambient waters was tested using a Fisher t-test (Fisher 1921). In this test, the statistic (t) is computed as the difference between the slopes of each correlation divided by the standard error of the difference between those slopes.

A fully factorial model III analysis of variance (ANOVA) was used to test for differences in both $\delta^{13}\text{C}$ -DIC and $\Delta^{14}\text{C}$ -DIC between the wet and dry seasons, and riverine and seawater end-member values. Averaged values are reported as arithmetic means \pm 1 SD, and differences were considered statistically significant at $P \leq 0.05$. Except where indicated, all statistical analyses were conducted using SAS version 9.1.3 (© 2000–2004 SAS Institute Inc., Cary, North Carolina, USA).

A first-order estimate of the contribution of terrestrially derived DIC to the isotopic signature recorded in coral skeleton was made for both the wet and dry season using a simple two end-member mass-balance equation:

$$\delta^{13}\text{C}_{\text{coral}} = x\delta^{13}\text{C}_{\text{FW}} + (1 - x)\delta^{13}\text{C}_{\text{SW}} \quad (1)$$

In this equation, x is the unknown proportion being solved for, $\delta^{13}\text{C}_{\text{coral}}$ represents average detrended $\delta^{13}\text{C}$ minima (wet season) and maxima (dry season) for the entire coral skeletal record, $\delta^{13}\text{C}_{\text{FW}}$ represents the average freshwater end-member $\delta^{13}\text{C}$ -DIC values measured in the Rio Fajardo (river and river mouth sites) during the wet or dry season, and $\delta^{13}\text{C}_{\text{SW}}$ represents the average marine end-member $\delta^{13}\text{C}$ -DIC values measured in the offshore waters adjacent to the Rio Fajardo catchment (bay and reef sites) during the wet or dry season. An error term for this estimate was calculated using standard arithmetic rules of propagation of uncertainty. By using the detrended coral $\delta^{13}\text{C}$ minima, any long-term trends present in the coral $\delta^{13}\text{C}$ were excluded from the mass-balance. Since metabolic fractionation effects were not directly measured, they cannot be accounted for in the mass-balance equation. A similar calculation was made for the $\Delta^{14}\text{C}$ of coral skeleton and DIC; however, due to the radiogenic nature and presence of bomb ^{14}C , a reliable estimate could not be obtained and is therefore not reported.

Results

Coral growth and chronology

X-radiographs of the Fajardo coral skeleton showed that only the top two sections of the core were oriented parallel to growth axis. Therefore, only these two core sections (total length = 32.3 cm) were used for further data analysis. In total, 56 distinct annual density band couplets

(1 couplet = 1 high- and 1 low-density band) were identified, spanning the period from 1948 to 2004 (Fig. 2). The high density portion of the coral skeleton is visible near the very top of the core (2004), indicating early to mid-summer deposition of this portion of the skeleton. The age model developed via density band counting agreed well with ^{14}C measurements (described in the following section) and no adjustments to the age model were necessary. The annual maximum linear skeletal extension (MLSE) ranged from 3.8 to 8.1 mm year⁻¹ with a mean annual MLSE rate of 5.72 ± 1.20 mm year⁻¹. Thus, on average, each coral $\delta^{13}\text{C}$ sample represents 2 months of coral growth. The coral $\delta^{13}\text{C}$ samples measured at 0.1-mm increments corresponded to the years 2002–2004 and each represented approximately 1 week of coral growth.

Coral skeletal $\delta^{13}\text{C}$ and $\Delta^{14}\text{C}$

Coral $\delta^{13}\text{C}$ values ranged from -3.12 to 0.44‰ and had an overall average of $-1.01 \pm 0.65\text{‰}$ (Fig. 3). Average annual $\delta^{13}\text{C}$ decreased at a rate of 0.018‰ year^{-1} over the span of the record (Fig. 3). Single spectrum analysis revealed a high spectral density with annual periodicity for the entire coral $\delta^{13}\text{C}$ record. Annual $\delta^{13}\text{C}$ minima typically occurred in the latter half of each year (range = June to January), and occurred most frequently during late November through early December. Average annual $\delta^{13}\text{C}$ minima ($-1.62 \pm 0.58 \text{‰}$) were significantly lower than average annual maxima ($-0.51 \pm 0.42\text{‰}$; $t_{\text{stat}} = -13.486$, $df = 55$, $P < 0.001$). Detrended high-resolution coral $\delta^{13}\text{C}$ anomalies ranged from -1.89 to 1.52‰ and averaged $-0.06 \pm 0.88\text{‰}$ (Fig. 4). The maximum value of the high-resolution $\delta^{13}\text{C}$ range was $\sim 1\text{‰}$ higher than that of the low-resolution data over the same time period, while

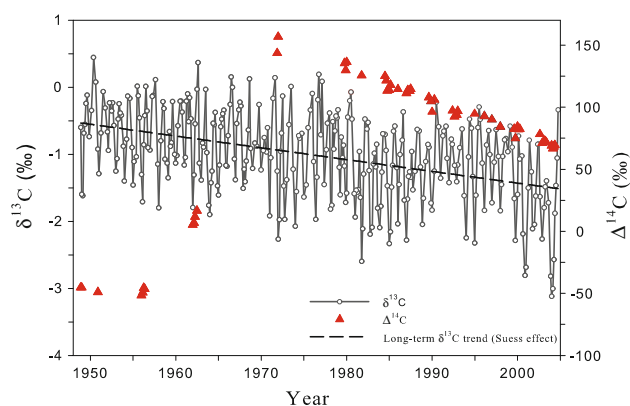


Fig. 3 $\delta^{13}\text{C}$ (open circle) and $\Delta^{14}\text{C}$ (filled triangle) values in the Fajardo coral core (1948–2004). The long-term $\delta^{13}\text{C}$ -Suess Effect (black dashed line) is also shown

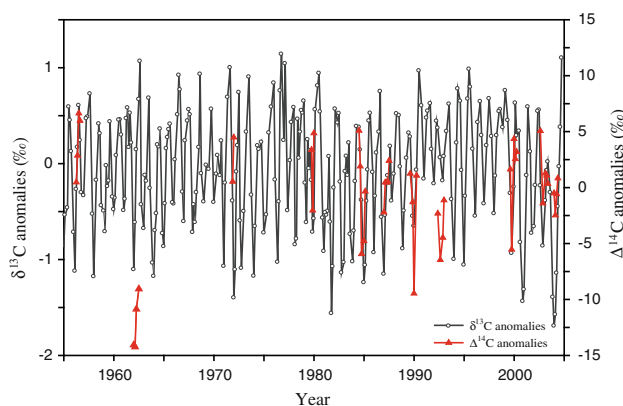


Fig. 4 $\delta^{13}\text{C}$ (open circle) and $\Delta^{14}\text{C}$ (filled triangle) anomalies in the Fajardo coral core for the period 1955–2004. $\delta^{13}\text{C}$ Suess effect was removed to generate $\delta^{13}\text{C}$ anomalies and the bomb radiocarbon trend was removed to generate $\Delta^{14}\text{C}$ anomalies

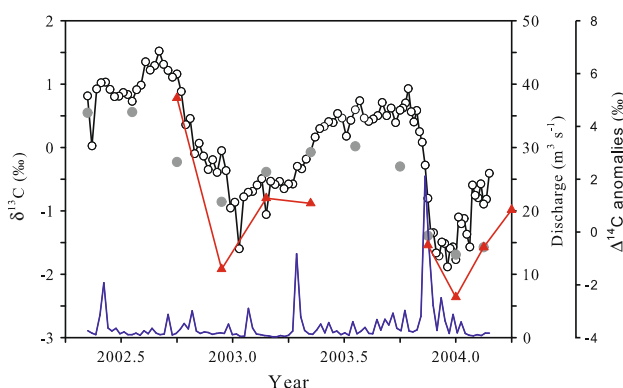


Fig. 5 High-resolution (0.1 mm) (open circle) and bi-monthly (filled circle) $\delta^{13}\text{C}$ in the Fajardo coral core for the period 2002–2004. Smoothed (weekly) Rio Fajardo discharge (blue line) and coral $\Delta^{14}\text{C}$ (filled triangle) anomalies are also shown

the minimum values of the two data sets were nearly identical (Fig. 5).

Cross-spectral analysis of Rio Fajardo discharge and the coral $\delta^{13}\text{C}$ time series revealed significant annual coherence (0.822, $P = 0.05$; Fig. 6). The two variables exhibited a near anti-phase relationship (phase angle = 178°), such that as discharge increased coral $\delta^{13}\text{C}$ anomalies decreased. Mass balance calculations revealed that during the wet season the proportionate contribution of land-derived $\delta^{13}\text{C}$ -DIC to the coral skeletal $\delta^{13}\text{C}$ minima was $24.8 \pm 4\%$. During the dry season, the proportionate contribution of land-derived $\delta^{13}\text{C}$ -DIC to the coral $\delta^{13}\text{C}$ maxima values was $16.8 \pm 8\%$.

The coral $\Delta^{14}\text{C}$ record exhibited a clear bomb ^{14}C signature (Fig. 3). Average $\Delta^{14}\text{C}$ decreased by 6‰ from 1948 to 1956 (-0.8‰ year^{-1}), increased by 208‰ from 1956 to 1972 (13‰ year^{-1}), and then decreased by 87‰ from 1972 to 2004 (-2.7‰ year^{-1}) (Fig. 3). Synchronous depletions

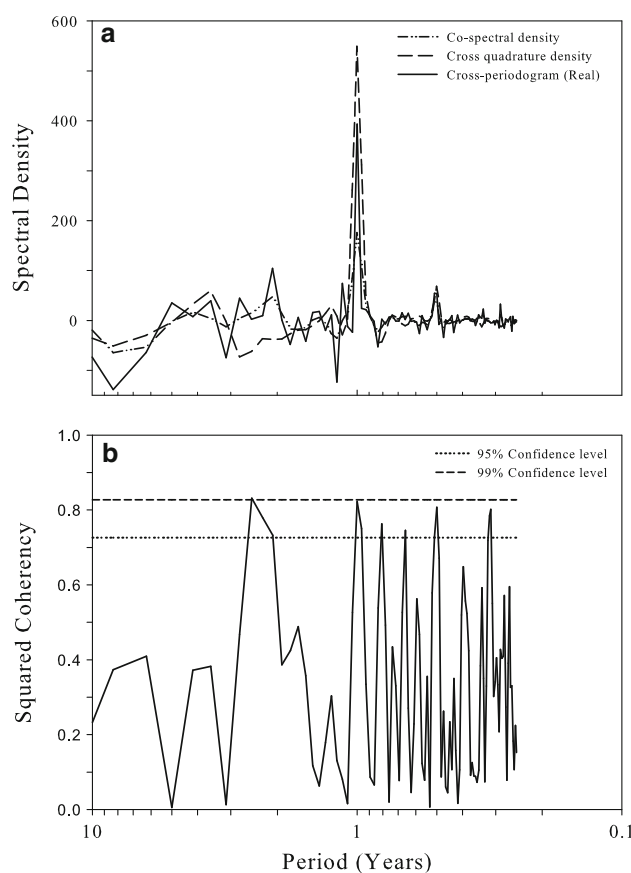


Fig. 6 Results of cross-spectral analysis between Rio Fajardo discharge and coral skeletal $\delta^{13}\text{C}$ anomalies during the period 1961 to 2004. **a** Spectral density estimates of the cross-spectrum (co-spectral and cross-quadrature densities) and the smoothed cross-periodogram. **b** Squared coherency of the two time series

of both $\delta^{13}\text{C}$ and $\Delta^{14}\text{C}$ anomalies were present for the periods 1955 to 1960 and again from 1975 to 2004 (Fig. 4). During the period of maximum bomb ^{14}C increase from 1960–1975 in the Fajardo coral (Fig. 4), no clear relationship between the coral skeletal $\delta^{13}\text{C}$ and $\Delta^{14}\text{C}$ anomalies was detected. Coral skeletal $\delta^{13}\text{C}$ and $\Delta^{14}\text{C}$ anomalies were positively correlated ($r = 0.444$; $P = 0.004$; Fig. 7).

DIC $\delta^{13}\text{C}$ and $\Delta^{14}\text{C}$

$\delta^{13}\text{C}$ -DIC values ranged from -9.82 to 0.93‰ (Table 1). Average freshwater (upriver and river mouth) values were significantly more depleted than average seawater (bay and reef) values (Table 2). In addition, average wet season $\delta^{13}\text{C}$ -DIC was lower than average dry season $\delta^{13}\text{C}$ -DIC; however, this difference was not statistically significant (Table 2). $\Delta^{14}\text{C}$ -DIC values ranged from 20.6 to 78.3‰ (Table 1), and average freshwater $\Delta^{14}\text{C}$ -DIC was significantly more depleted than average seawater $\Delta^{14}\text{C}$ -DIC (Table 2). Average wet season $\Delta^{14}\text{C}$ -DIC was also significantly higher than corresponding average dry season

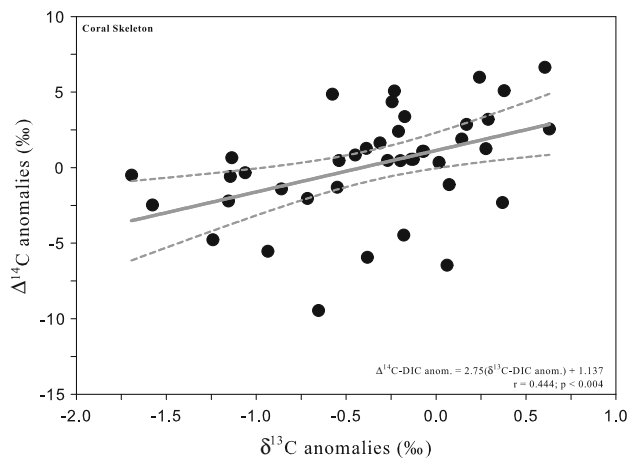


Fig. 7 Fajardo coral skeletal $\delta^{13}\text{C}$ versus $\Delta^{14}\text{C}$ anomalies. The linear correlation = *solid gray line*; 95% confidence intervals = *gray dashed lines*

$\Delta^{14}\text{C}$ -DIC (Table 2). $\delta^{13}\text{C}$ -DIC and $\Delta^{14}\text{C}$ -DIC were positively correlated ($r = 0.842$; $P < 0.001$; Fig. 8). The slope of this correlation was not significantly different from the slope of the correlation between coral skeletal $\delta^{13}\text{C}$ and $\Delta^{14}\text{C}$ anomalies ($t_{\text{stat}} = 0.82$, $\text{df} = 60$, $P \leq 0.05$).

Discussion

Coral growth

The average MLSE rate measured in the Fajardo core (5.2 mm year^{-1}) is much lower than those reported for *Montastraea* sp. elsewhere in the Caribbean region. Shallow water (1–10 m) *Montastraea* sp. corals have annual growth ranging from 7 to 10 mm year^{-1} , with MLSE rates of *M. faveolata* typically being on the high end of that range (Gladfelter et al. 1978; Hubbard and Scaturo 1985; Risk et al. 1992; Carricart-Ganivet et al. 2000; Moses and Swart 2006). The observed MLSE was more similar to that of *M. annularis* complex corals reported from depths of 14 m at Tobago (Moses and Swart 2006), 18–37 m at St. Croix (Hubbard and Scaturo 1985), and 44 m at Barbados (Runnalls and Coleman 2003). Since Cayo Ahogado is located at a shallow embayment $\sim 1 \text{ km}$ from the mouth of the Rio Fajardo, sedimentation and turbidity are likely major factors limiting coral growth rates on the reef. Several studies have attributed slow growth rates of *Montastraea* sp. to terrigenous sedimentation at other locations within Puerto Rico (Loya 1976; Morelock et al. 1983; Torres and Morelock 2002). Sediment yields from small mountainous rivers, such as the Rio Fajardo, are known to be large (Milliman and Syvitski 1992), and are therefore capable of producing turbid conditions that would slow or limit coral growth. Secchi depth measurements made

during water collections never exceeded 4.0 m, and the seafloor (max. depth = 7 m) was never visible during sampling. Therefore, the reduced growth rates observed in the Fajardo core are likely due to the coral growing in turbid waters, and indicate a physical link between river discharge and corals growing at Cayo Ahogado.

Coral skeletal $\delta^{13}\text{C}$ and $\Delta^{14}\text{C}$

The observed decrease in mean $\delta^{13}\text{C}$ over the span of the 56-year coral record (-0.018‰ year^{-1} ; Fig. 3) is consistent with the observed rate of decrease in tropical atmospheric $\delta^{13}\text{C}$ (-0.02‰ year^{-1}) over the same time period (Keeling et al. 2005). The similarity in depletion rates between the coral and atmospheric $\delta^{13}\text{C}$ records strongly suggest that the so-called ^{13}C -Suess effect is driving the long-term average $\delta^{13}\text{C}$ decrease observed in the Fajardo core. Such agreement between global trends in atmospheric and coral skeletal $\delta^{13}\text{C}$ has recently been reported by Swart et al. (2010). Annual periodicity of $\delta^{13}\text{C}$ was present in the Fajardo coral record (Figs. 4, 5, 6) and has been reported for *M. faveolata* in the Caribbean and western Atlantic region (Fairbanks and Dodge 1979; Halley et al. 1994; Swart et al. 1996), although the timing of annual $\delta^{13}\text{C}$ maxima and minima varies among geographic locations and individual records. This has given rise to a range of different interpretations as to the source of annual $\delta^{13}\text{C}$ variation in coral skeletal records (see reviews by Swart 1983; Swart et al. 1996; Grottoli 2000).

The timing of the annual $\delta^{13}\text{C}$ maxima (early summer) and minima (very late autumn) reported here do not coincide with those reported in Florida (max. = mid-spring, min. = mid-summer) (Swart et al. 1996), and occur just prior to those reported in Barbados and Jamaica (max. = mid-summer, min. = early winter) (Fairbanks and Dodge 1979). Watanabe et al. (2002) reported the occurrence of $\delta^{13}\text{C}$ maxima in early summer from corals collected off the southwest coast of Puerto Rico (La Parguera); however, the occurrence of the $\delta^{13}\text{C}$ minima in those cores was highly variable and ranged from late summer to spring of the following year. At their study site, no direct inputs of riverine DIC are present, and the variability in coral skeletal $\delta^{13}\text{C}$ was attributed to variations in cloud cover (Watanabe et al. 2002). In the Fajardo coral, $\delta^{13}\text{C}$ minima occur at nearly the same time each year (very late autumn) over the entire record (Fig. 4) and correspond well with increases in river discharge during the wet season (Fig. 6). Thus, variations in coral skeletal $\delta^{13}\text{C}$ indicate control by local inputs of low $\delta^{13}\text{C}$ riverine DIC.

The long-term trend in coral skeletal $\Delta^{14}\text{C}$ was clearly driven by the influx of bomb ^{14}C (Fig. 3). Both the amount (157‰) and occurrence of peak bomb ^{14}C values measured in the 1972 growth band of the Fajardo coral are consistent

Table 1 Stable ($\delta^{13}\text{C}$) and radiocarbon ($\Delta^{14}\text{C}$) isotope ratios measured in the dissolved inorganic carbon (DIC) of river and seawater at the Rio Fajardo catchment in eastern Puerto Rico

Location	Date	Salinity (‰)	$\delta^{13}\text{C}$ -DIC (‰, VPDB)	$\Delta^{14}\text{C}$ -DIC (‰)
Upriver	October 2004	0.0	-8.76	59.4
	October 2007	0.0	-9.82	49.8
	March 2005	0.0	-8.23	26.9
	March 2008	0.1	-9.02	27.4
River mouth	October 2004	8.0	-3.34	59.2
	October 2007	2.0	-8.24	46.2
	March 2005	17.0	-6.34	20.6
	March 2008	11.1	-6.20	40.3
Nearshore	October 2007	17.0	0.03	67.8
	March 2008	35.8	0.62	62.9
Bay	October 2004	36.0	0.66	71.2
	October 2007	26.0	0.87	70.9
	March 2005	36.0	0.89	65.1
	March 2008	36.1	0.91	71.6
Reef	October 2004	34.5	0.71	78.3
	October 2007	36.0	0.92	73.9
	March 2005	38.0	0.93	70.7
	March 2008	35.5	0.86	68.1

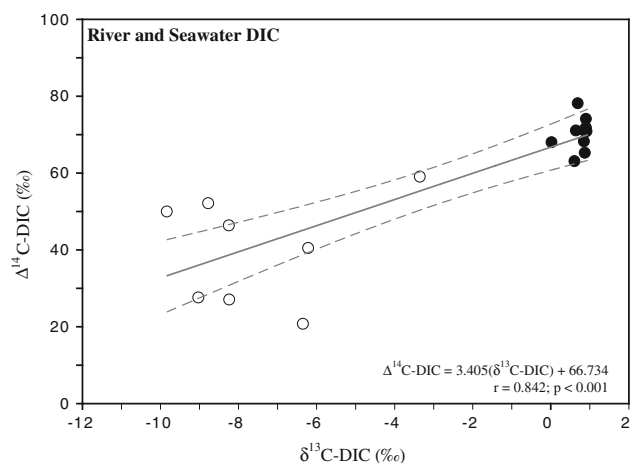
Sampling date and salinity at the time of sampling are also given

Table 2 Results of a fully factorial 2-way model III analysis of variance (ANOVA) to test for the effect of salinity (fresh vs. marine) and season (wet vs. dry) on both $\delta^{13}\text{C}$ -DIC and $\Delta^{14}\text{C}$ -DIC values

$\delta^{13}\text{C}$ -DIC	df	SS	F	P	$\Delta^{14}\text{C}$ -DIC	df	SS	F	P
Model	3	301.49	153.54	<0.001	Model	3	4879.23	48.78	<0.001
Salinity	1	301.45	460.56	<0.001	Salinity	1	3600.00	107.98	<0.001
Season	1	2.38	3.64	0.0828	Season	1	873.20	26.19	<0.001
Salinity*Season	1	1.74	2.70	0.1287	Salinity*Season	1	406.02	12.18	<0.005

Only end-member values (i.e., upriver and reef) were used in this analysis

df degrees of freedom, SS sum of squares, F calculated F statistic, P probability. Sources of variability are significant when $P \leq 0.05$

**Fig. 8** Rio Fajardo (open circle) and coastal seawater (filled circle) $\delta^{13}\text{C}$ -DIC versus $\Delta^{14}\text{C}$ -DIC. Linear correlation = solid gray line; 95% confidence intervals = gray dashed lines

with published values ($\sim 160\text{‰}$ and 1970–1975, respectively) from other coral records in the western Atlantic/eastern Pacific region of the Northern Hemisphere (Grottoli and Eakin 2007). Additionally, the rate of increase of bomb ^{14}C within the Fajardo coral (13.01‰ year^{-1}) falls within the range ($5.81\text{--}18.99\text{‰ year}^{-1}$) of those reported by Grottoli and Eakin (2007) for corals growing in the western Atlantic/eastern Pacific region of the Northern Hemisphere.

Relationship between river discharge and coral skeletal $\delta^{13}\text{C}$ and $\Delta^{14}\text{C}$

First-order mass-balance calculations show that as much as 25% of the $\delta^{13}\text{C}$ signature of the Fajardo coral skeleton may be influenced by riverine DIC inputs during the wet season. Conversely in the dry season, 17% of the $\delta^{13}\text{C}$ signature may be derived from riverine DIC. Thus, the

seasonal periodicity of riverine DIC input to the coastal ocean is likely influencing the annual periodicity observed in coral skeletal $\delta^{13}\text{C}$, with lower coral $\delta^{13}\text{C}$ corresponding to the occurrence of the wet season. The relatively small difference between seasonal contributions of riverine DIC to the coral skeletal $\delta^{13}\text{C}$ signature is likely a result of the relatively small contribution of riverine discharge in both seasons to the much larger ocean DIC pool. As such, coral skeletal $\delta^{13}\text{C}$ alone cannot be used to distinguish whether the observed depletions are a result of increased riverine DIC input to coastal ocean, the result of metabolic fractionation effects brought about by associated wet season phenomena (e.g., increased heterotrophy, cloud cover, or turbidity), or some combination of both.

Although an increase in heterotrophy or a decrease in ambient light driven by increase in cloud cover or turbidity during the wet season can also drive skeletal $\delta^{13}\text{C}$ toward more negative values (e.g., Grottoli and Wellington 1999), neither increased heterotrophy nor decreased light would produce a change in the $\Delta^{14}\text{C}$ of the coral skeleton. In the Fajardo core, skeletal $\delta^{13}\text{C}$ and $\Delta^{14}\text{C}$ exhibit synchronous depletions coincident with increases in river discharge (Figs. 4, 6), suggesting a non-metabolic influence on the $\delta^{13}\text{C}$ and $\Delta^{14}\text{C}$ of the coral skeleton brought about by changes in surrounding DIC and corals during the wet season. These synchronous depletions primarily occur within the low-density portion of the annual growth bands, immediately following the deposition of the high-density portion of the annual band. According to the age model, these negative $\delta^{13}\text{C}$ and $\Delta^{14}\text{C}$ excursions occur between the months of October and January, which is coincident with the timing of the wet season in the Rio Fajardo catchment. The inverse relationship between coral skeletal $\delta^{13}\text{C}$ and river discharge (Fig. 6) coupled with the synchronous depletion of both $\delta^{13}\text{C}$ and $\Delta^{14}\text{C}$ in the coral skeleton are evidence that riverine DIC is influencing the carbon isotopic signature of the Fajardo coral during the wet season.

Comparison of coral skeletal $\delta^{13}\text{C}$ anomalies analyzed at both high- and low resolution (0.1 mm and 1.0 mm, respectively) over an approximately 2-year period of Fajardo coral growth reveals the same pattern of seasonal $\delta^{13}\text{C}$ variability for both records (Fig. 5). However, the high-resolution record exhibited a higher amplitude and greater intra-annual variability. These findings are consistent with other studies that have examined sampling resolution as a consideration of coral isotope interpretation in the *Montastraea sp.* complex (Halley et al. 1994; Leder et al. 1996; Watanabe et al. 2002; Smith et al. 2006). Given the links between freshwater DIC delivery and coral carbon isotopes, it was expected that high-resolution $\delta^{13}\text{C}$ measurements could help identify individual river discharge events (i.e., floods). However, there was not always a clear

relationship between peaks in river discharge and decreases in coral skeletal $\delta^{13}\text{C}$ when the high-resolution $\delta^{13}\text{C}$ data were examined (Fig. 5). However, over longer-time intervals (monthly—seasonal), the general relationship between increased river discharge during the wet season and decreased coral skeletal $\delta^{13}\text{C}$ anomalies does hold (Fig. 6). These data indicate that either the processes governing the geochemistry of coral skeletons are not sensitive to single river discharge events, or samples analyzed at approximately weekly intervals do not have sufficient resolution to identify individual river discharge events. Furthermore, these data also demonstrate the importance of using paired measurements of $\delta^{13}\text{C}$ and $\Delta^{14}\text{C}$ to detect riverine influence in coral skeletons.

Relationship between DIC and coral skeletal isotopes

The influence of riverine DIC on the geochemistry of the Fajardo coral skeleton becomes more apparent when examined in the context of the $\delta^{13}\text{C}$ -DIC and $\Delta^{14}\text{C}$ -DIC values (Table 1). The slopes of the correlations between $\delta^{13}\text{C}$ and $\Delta^{14}\text{C}$ anomalies in the coral skeleton (Fig. 7) and seawater $\delta^{13}\text{C}$ -DIC and $\Delta^{14}\text{C}$ -DIC (Fig. 8) were not significantly different, and both $\delta^{13}\text{C}$ and $\Delta^{14}\text{C}$ were lower in riverine versus coastal seawater DIC (Fig. 8). Thus, when large pulses of river water bathe the reef, the $\delta^{13}\text{C}$ -DIC and $\Delta^{14}\text{C}$ -DIC of those waters should decrease relative to open ocean seawater values. Since peak Rio Fajardo discharge occurs in November, the isotopic influence of riverine DIC in coastal seawater DIC should be most pronounced during that time. Other studies within Puerto Rico have also shown similar patterns in the annual variability of coastal seawater $\delta^{13}\text{C}$ -DIC. Watanabe et al. (2002) reported monthly $\delta^{13}\text{C}$ -DIC measurements from La Parguera, Puerto Rico over a 1.5-year period. Their results show DI- $\delta^{13}\text{C}$ values to be lower during the months of October and November, and higher from January through August. In their interpretation, the influence of $\delta^{13}\text{C}$ -depleted freshwater plumes emanating from the Orinoco River is cited as a source of the observed seasonality of $\delta^{13}\text{C}$ -DIC over local sources of depleted $\delta^{13}\text{C}$ -DIC. However, the data presented in this study suggest local sources of terrestrial DIC are highly capable of influencing the isotopic composition of coastal waters.

Since the Fajardo catchment is subject to seasonal climatic variability, it follows that most $\delta^{13}\text{C}$ and $\Delta^{14}\text{C}$ depleted freshwater would mix with coastal waters during the wet season. Moyer (2008) has shown that $\delta^{13}\text{C}$ -DIC and $\Delta^{14}\text{C}$ -DIC both mix conservatively from the Rio Fajardo to the reef at Cayo Ahogado during the wet season, but not during the dry season. This seasonal difference indicates that the $\delta^{13}\text{C}$ -DIC and $\Delta^{14}\text{C}$ -DIC waters bathing the reef at Cayo Ahogado are only influenced by riverine

input to the coastal ocean during the wet season. Accordingly, the $\delta^{13}\text{C}$ and $\Delta^{14}\text{C}$ signature of the coral skeleton is expected to record the influence of riverine DIC most faithfully at times when river discharge is large enough to cause conservative isotopic mixing between fresh and seawater DIC (i.e., during the wet season).

Conceptual model

A conceptual model is presented showing the sources of carbon to the Rio Fajardo and coastal ocean, the $\delta^{13}\text{C}$ and $\Delta^{14}\text{C}$ signature associated with the dominant carbon pools, how these relationships change with seasonal changes in river discharge, and how that ultimately influences the $\delta^{13}\text{C}$ and $\Delta^{14}\text{C}$ in the skeletal record (Fig. 9). The DIC $\delta^{13}\text{C}$ and $\Delta^{14}\text{C}$ values presented in the model are based on direct measurements made in this study (Table 1). The DOC and POC $\delta^{13}\text{C}$ and $\Delta^{14}\text{C}$ values are also based on direct measurements within the study area (Moyer 2008), and soil and plant OM isotope values in Puerto Rico were drawn from the published literature (von Fischer and Tieszen 1995; Marin-Spiotta et al. 2008).

A major source of DIC in riverine systems is the conversion of DOC and POC into DIC via both abiotic (e.g., photo-oxidation) and biotic (e.g., respiration) processes. Plant biomass and surface soils are the main sources of OM to rivers, and have $\delta^{13}\text{C}$ values reflective of the vegetation within the river catchment. In a primarily forested catchment such as Fajardo, plant OM has an average $\delta^{13}\text{C}$ value of -30‰ , and soil OM values range from -26 to -28‰ (von Fischer and Tieszen 1995). Soil OM ages significantly on land (e.g., Blair et al. 2003), and the majority of this aged OM is broken down in rivers and transported to the coastal ocean in the form of DOC (Hope et al. 1994). The fraction of aged soil OM that is not converted to DOC is transported to the coastal ocean as POC.

The conversion of DOC and POC into DIC in the river is reflected in the conceptual model (Fig. 9). The lack of pre-bomb $\Delta^{14}\text{C}$ in any of the DIC samples from this study indicates that the DIC exported to the reef in Fajardo is reflective of a source that represents a mixture of modern and old OM (Fig. 9). Since the Fajardo core was collected very near to shore at a location far from the shelf edge, upwelling can be ruled out as a factor controlling local $\Delta^{14}\text{C}$ variability. Regardless of the source of the DIC isotopic signature, both the $\delta^{13}\text{C}$ -DIC and $\Delta^{14}\text{C}$ -DIC of the Rio Fajardo were always lower than those of the coastal ocean surface waters (Table 1; Moyer 2008).

The seasonal component of riverine DIC influence to the coastal ocean, and ultimately the coral skeleton, is also reflected in the conceptual model (Fig. 9). During the wet season, riverine DIC isotopes mix conservatively along a salinity gradient caused by the river discharge plume

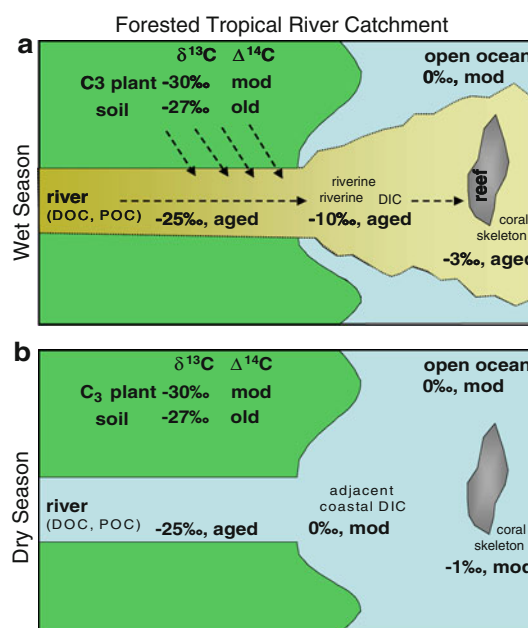


Fig. 9 Conceptual model showing the relationship between the major sources of carbon from within the Rio Fajardo catchment, the coastal ocean, and coral skeleton. Average $\delta^{13}\text{C}$ and relative ^{14}C ages are given for each of the dominant carbon pools. The $\delta^{13}\text{C}$ and $\Delta^{14}\text{C}$ values in river and coastal ocean DIC, and coral skeleton are shown for the wet (a) and dry (b) seasons. $\delta^{13}\text{C}$ and $\Delta^{14}\text{C}$ reflect measured (DIC, Table 1) or published values (soil, plants, DOC, and POC; von Fischer and Tieszen 1995; Marin-Spiotta et al. 2008; Moyer 2008). ^{14}C relative ages range from modern ('mod') to 'old', with intermediate values designated as 'aged'

(Fig. 9a; Moyer 2008). This same pattern does not hold true during the dry season when river discharge is generally diminished and riverine DIC does not, at least isotopically, mix conservatively across the salinity gradient (Fig. 9b; Moyer 2008). Therefore, coral $\delta^{13}\text{C}$ and $\Delta^{14}\text{C}$ are only shown to be affected by the isotopic signature of terrestrially derived DIC during the wet season, with the observed response being relative depletions in both $\delta^{13}\text{C}$ and $\Delta^{14}\text{C}$ within the coral skeleton.

Implications for coral proxy records

Given the influence of terrestrially derived DIC on coral skeletal $\delta^{13}\text{C}$ and $\Delta^{14}\text{C}$ values in the Fajardo core, the findings presented here have several implications for interpreting proxy records for palaeo-reconstructions. When skeletal $\delta^{13}\text{C}$ and $\Delta^{14}\text{C}$ are measured in tandem at sub-annual resolution, it is possible to resolve the seasonal influence of terrestrially derived DIC on coral skeletal geochemistry. This dual isotope approach allows for a much clearer distinction between coral $\delta^{13}\text{C}$ variability brought about by changes in the isotopic composition of DIC and those due to metabolic fractionation effects. The mass-balance calculations in this study indicate that as

much as 25% of the coral skeletal $\delta^{13}\text{C}$ signature may be derived from terrestrial DIC. This is an important consideration that must be accounted for when interpreting $\delta^{13}\text{C}$ data from corals living in coastal settings with local freshwater inputs.

The use of multi-proxy records including $\delta^{13}\text{C}$ and $\Delta^{14}\text{C}$ in combination with other known tracers of riverine input such as Ba/Ca or other trace elements (Alibert et al. 2003; McCulloch et al. 2003; Lewis et al. 2007; Prouty et al. 2009), or luminescence (Isdale 1984; Grove et al. 2010), could help provide historical records of riverine carbon input to reefs, in terms of both DIC and POC. However, additional controlled experimental studies are necessary in order to make this dual carbon isotope method a fully quantitative proxy for estimating carbon flux to the coastal ocean. With additional experimental calibration, such records could be used as proxies for the history of land–ocean carbon flux for many areas of the tropics where river discharge data are few, and local river–ocean carbon fluxes are not well understood. Such a proxy would be extremely useful in helping to gain a clearer understanding of historical dynamics in tropical land–ocean carbon flux in the context of modern global climate change and land-use change practices.

Acknowledgments AGG was supported by grants from the Andrew Mellon Foundation and the NSF Chemical Oceanography Program (OCE-0610487). RPM was a graduate student in Grottoli's lab, and partially supported by an OSU Presidential Fellowship. RPM received additional funding from AAPG, AGU, GSA, and the Friends of Orton Hall, and was supported by a USGS Mendenhall Fellowship during manuscript preparation. Field assistance was provided by H. Anguerre, M. Canals, M. Cathey, C. Malachowski, C. Pacheco, and B. Williams. Coral x-radiography was facilitated by K. Helmlé and R. Dodge at the NSU Oceanographic Center. Laboratory assistance was provided by M. Cathey, Y. Matsui, C. Paver, L. Swierk, and H. Wu, and L. Travers assisted with figure preparation. J. Bauer, A. Carey, Y-P. Chin, N. Prouty, B. Rosenheim, M. Saltzman, B. Williams, and an anonymous person provided careful reviews and suggestions which improved the overall quality of the manuscript. Any use of trade names is for descriptive purposes only and does not imply endorsement by the US Government.

References

- Alibert C, Kinsley L, Fallon SJ, McCulloch MT, Berkemans R, McAllister F (2003) Source of trace element variability in Great Barrier Reef corals affected by the Burdekin flood plumes. *Geochim Cosmochim Acta* 67:231–246
- Blair NE, Leithold EL, Ford ST, Peeler KA, Holmes JC, Perkey DW (2003) The persistence of memory: the fate of ancient sedimentary organic carbon in a modern sedimentary system. *Geochim Cosmochim Acta* 67:63–73
- Carricart-Ganivet JP, Beltrán-Torres AU, Merino M, Ruiz-Zarate MA (2000) Skeletal extension, density and calcification rate of the reef building coral *Montastrea annularis* (Ellis and Solander) in the Mexican Caribbean. *Bull Mar Sci* 66:215–224

- Coplen TB (1996) New guidelines for reporting stable hydrogen, carbon, and oxygen isotope-ratio data. *Geochim Cosmochim Acta* 60:3359–3360
- Dodge RE, Vaisnys JR (1975) Hermatypic coral growth banding as environmental recorder. *Nature* 258:706–708
- Druffel ERM (1997) Geochemistry of corals: proxies of past ocean chemistry, ocean circulation, and climate. *Proc Natl Acad Sci USA* 94:8354–8361
- Druffel EM, Linick TW (1978) Radiocarbon in annual coral rings of Florida. *Geophys Res Lett* 5:913–916
- Eakin CM, Grottoli AG (2006) Paleo-climate changes and corals. In: Phinney J, Skirving W, Kleypas J, Hoegh-Guldberg O, Strong AE (eds) *Coral reefs and climate change: science and management*. Coastal and Estuarine Studies 61:33–54
- Fairbanks RG, Dodge RE (1979) Annual periodicity of the $^{18}\text{O}/^{16}\text{O}$ and $^{13}\text{C}/^{12}\text{C}$ ratios in the coral *Montastrea annularis*. *Geochim Cosmochim Acta* 43:1009–1020
- Fisher RA (1921) On the probable error of a coefficient of correlation deduced from a small sample. *Metron* 1:3–32
- Furla P, Galgani I, Durand I, Allemand D (2000) Sources and mechanisms of inorganic carbon transport for coral calcification and photosynthesis. *J Exp Biol* 203:3445–3457
- Gagan MK, Ayliffe LK, Beck JW, Cole JE, Druffel ERM, Dunbar RB, Schrag DP (2000) New views of tropical paleoclimates from corals. *Quaternary Sci Rev* 19:45–64
- Gladfelter EH, Monahan RK, Gladfelter WB (1978) Growth rates of five reef-building corals in the northeastern Caribbean. *Bull Mar Sci* 28:728–734
- Grottoli AG (2000) Stable carbon isotopes ($\delta^{13}\text{C}$) in coral skeletons. *Oceanography* 13:93–97
- Grottoli AG (2002) Effect of light and brine shrimp levels on skeletal $\delta^{13}\text{C}$ values in the Hawaiian coral *Porites compressa*: a tank experiment. *Geochim Cosmochim Acta* 66:1955–1967
- Grottoli AG, Eakin CM (2007) A review of modern coral $\delta^{18}\text{O}$ and $\Delta^{14}\text{C}$ proxy records. *Earth-Sci Rev* 81:67–91
- Grottoli AG, Wellington GM (1999) Effect of light and zooplankton on skeletal $\delta^{13}\text{C}$ values in the eastern Pacific corals *Pavona clavus* and *Pavona gigantea*. *Coral Reefs* 18:29–41
- Grove CA, Nagtegaal R, Zinke J, Scheufen T, Koster B, Kasper S, McCulloch MT, van den Bergh G, Brummer GJA (2010) River runoff reconstructions from novel spectral luminescence scanning of massive coral skeletons. *Coral Reefs* 29:579–591
- Halley RB, Swart PK, Dodge RE, Hudson JH (1994) Decade-scale trend in sea water salinity revealed through $\delta^{18}\text{O}$ analysis of *Montastrea annularis* annual growth bands. *Bull Mar Sci* 54:670–678
- Heikoop JM, Dunn JJ, Risk MJ, Schwarcz HP, McConnaughey TA, Sandeman IM (2000) Separation of kinetic and metabolic isotope effects in carbon-13 records preserved in reef coral skeletons. *Geochim Cosmochim Acta* 64:975–987
- Hope D, Billett MF, Cresser MS (1994) A review of the export of carbon in river water: fluxes and processes. *Environ Pollut* 84:301–324
- Hubbard DK, Scaturro D (1985) Growth rates of seven species of scleractinian corals from Cane Bay and Salt River, St. Croix, USVI. *Bull Mar Sci* 36:325–338
- Hudson JH, Shinn EA, Halley RB, Lidz B (1976) Sclerochronology—A tool for interpreting past environments. *Geology* 4:360–364
- Hughes AD, Grottoli AG, Pease TK, Matsui Y (2010) The acquisition and utilization of carbon in non-bleached and bleached corals. *Mar Ecol Prog Ser* 420:91–101
- Isdale PJ (1984) Fluorescent bands in massive corals record centuries of coastal rainfall. *Nature* 310:578–579
- Keeling CD, Bollenbacher AF, Whorf TP (2005) Monthly atmospheric $^{13}\text{C}/^{12}\text{C}$ isotopic ratios for 10 SIO stations. In: Trends A (ed) *Compendium of data on global change*. Carbon Dioxide

- Information Analysis Center, Oak Ridge National Laboratory, US Department of Energy, Oak Ridge, Tenn, USA. <http://cdiac.esd.ornl.gov/trends/co2/iso-sio/iso-sio.html>
- Kilbourne KH, Quinn TM, Guilderson TP, Webb RS, Taylor FW (2007) Decadal- to interannual-scale source water variations in the Caribbean Sea recorded by Puerto Rican coral radiocarbon. *Clim Dynam* 29:51–62
- Klein R, Patzold J, Wefer G, Loya Y (1992) Seasonal variations in the stable isotopic composition and the skeletal density pattern of the coral *Porites lobata* (Gulf of Eilat, Red Sea). *Mar Biol* 112:259–263
- Knutson DW, Buddemeier RW, Smith SV (1972) Coral chronometers: seasonal growth bands in reef corals. *Science* 177:270–272
- Konishi K, Tanaka T, Sakanoue M (1982) Secular variation of radiocarbon concentration in seawater: sclerochronological approach. *Proc 4th Int Coral Reef Symp* 1:181–185
- Leder JJ, Swart PK, Szmant AM, Dodge RE (1996) The origin of variations in the isotopic record of scleractinian coral: I. Oxygen. *Geochim Cosmochim Acta* 60:2857–2870
- Lewis SE, Shields GA, Kamber BS, Lough JM (2007) A multi-trace element coral record of land-use changes in the Burdekin River catchment, NE Australia. *Palaeogeogr Palaeoclimatol Palaeoecol* 246:471–487
- Loya Y (1976) Effects of water turbidity and sedimentation on the community structure of Puerto Rico corals. *Bull Mar Sci* 26:450–466
- Lyons WB, Nezat AC, Carey AE, Hicks DM (2002) Organic carbon fluxes to the ocean from high-standing islands. *Geology* 30:443–446
- Marin-Spiotta E, Swanston CW, Torn MS, Silver WL, Burton SD (2008) Chemical and mineral control of soil carbon turnover in abandoned tropical pastures. *Geoderma* 143:49–62
- Mayorga E, Aufdenkampe AK, Masiello CA, Krusche AV, Hedges JI, Quay PD, Richey JE, Brown TA (2005) Young organic matter as a source of carbon dioxide outgassing from Amazonian rivers. *Nature* 436:469–470
- McCulloch MT, Fallon SJ, Wyndham T, Hendy EJ, Lough JM, Barnes DJ (2003) Coral record of increased sediment flux to the inner Great Barrier Reef since European settlement. *Nature* 421:727–730
- Milliman JD, Syvitski JPM (1992) Geomorphic/tectonic control of sediment discharge to the ocean: the importance of small mountainous rivers. *Geology* 100:525–544
- Morelock J, Grove K, Hernández ML (1983) Oceanography and patterns of shelf sediments Mayagüez, Puerto Rico. *J Sediment Petrol* 53:31–381
- Moses CS, Swart PK (2006) Stable isotope and growth records in corals from the island of Tobago: not simply a record of the Orinoco. *Proc 10th Int Coral Reef Symp* 1:580–587
- Moyer RP (2008) Carbon isotopes and trace elements in small mountainous rivers and coastal coral skeletons in Puerto Rico. Ph.D. thesis, The Ohio State University, pp 43–102
- Muscantine L, Porter JW, Kaplan IR (1989) Resource partitioning by reef corals as determined from stable isotope composition. *Mar Biol* 100:85–193
- Nozaki Y, Rye DM, Turekian KK, Dodge RE (1978) 200 year record of carbon-13 and carbon-14 variations in a Bermuda coral. *Geophys Res Lett* 5:825–828
- Prouty NG, Jupiter SD, Field ME, McCulloch MT (2009) Coral proxy record of decadal-scale reduction in base flow from Moloka'i, Hawaii. *Geochem Geophys Geosys* 10:Q12018. doi:10.1029/2009GC002714
- Raymond PA, Bauer JE (2001) Use of ^{14}C and ^{13}C natural abundances for evaluating riverine, estuarine, and coastal DOC and POC sources and cycling: a review and synthesis. *Org Geochem* 32:469–485
- Reynaud-Vaganay S, Juillet-Leclerc A, Jaubert J, Gattuso J-P (2001) Effect of light on skeletal $\delta^{13}\text{C}$ and $\delta^{18}\text{O}$, and interaction with photosynthesis, respiration and calcification in two zooxanthellate scleractinian corals. *Palaeogeogr Palaeoclimatol Palaeoecol* 175:393–404
- Risk MJ, Van Wissen FA, Beltran JC (1992) Sclerochronology of Tobago corals: a record of the Orinoco? *Proc 7th Int Coral Reef Symp* 1:156–161
- Runnalls LA, Coleman ML (2003) Record of natural and anthropogenic changes in reef environments (Barbados West Indies) using laser ablation ICP-MS and sclerochronology on coral cores. *Coral Reefs* 22:416–426
- Smith JM, Quinn TM, Helmle KP, Halley RB (2006) Reproducibility of geochemical and climatic signals in the Atlantic coral *Montastraea faveolata*. *Paleoceanography* 21: PA1010. doi:10.1029/2005PA001187
- Stuiver M, Polach HA (1977) Discussion: reporting of ^{14}C data. *Radiocarbon* 19:355–363
- Swart PK (1983) Carbon and oxygen isotope fractionation in scleractinian corals: a review. *Earth Sci Rev* 19:51–80
- Swart PK, Leder JJ, Szmant A, Dodge RE (1996) The origin of variations in the isotopic record of scleractinian Corals: II. Carbon. *Geochim Cosmochim Acta* 60:2871–2886
- Swart PK, Szmant Porter JW, Dodge RE, Tougas JI, Southam JR (2005) The isotopic composition of respired carbon dioxide in scleractinian corals: implications for cycling of organic carbon in corals. *Geochim Cosmochim Acta* 69:1495–1509
- Swart PK, Greer L, Rosenheim BE, Moses CS, Waite AJ, Winter A, Dodge RE, Helmle KP (2010) The ^{13}C Suess effect in scleractinian corals mirror changes in the anthropogenic CO_2 inventory of the surface oceans. *Geophys Res Lett* 37:L05604. doi:10.1029/2009GL041397
- Thompson RORY (1979) Coherence significance levels. *J Atmos Sci* 36:2020–2021
- Torres JL, Morelock J (2002) Effect of terrigenous sediment influx on coral cover and linear extension rates of three Caribbean massive coral species. *Caribb J Sci* 38:222–229
- Vogel JS, Southon JR, Nelson DE (1987) Catalyst and binder effects in the use of filamentous graphite for AMS. *Nuclear Instrumentation and Methods Physics Research B* 29:50–56
- von Fischer JC, Tieszen LL (1995) Carbon isotope characterization of vegetation and soil organic matter in subtropical forests in Luquillo, Puerto Rico. *Biotropica* 27:138–148
- Watanabe T, Winter A, Oba T, Anzai R, Ishioroshi H (2002) Evaluation of the fidelity of isotope records as an environmental proxy in the coral *Montastraea*. *Coral Reefs* 21:169–178